Korean J. Chem. Eng., 32(8), 1655-1666 (2015)
DOI: 10.1007/s11814-014-0351-5

pISSN: 0256-1115
eISSN: 1975-7220

Adsorption of malachite green in aqueous solution onto sodium carbonate treated rice husk

Binod Kumar and Upendra Kumar†

Department of Civil Engineering, National Institute of Technology, Silchar, Assam, India
(*Received 13 September 2014 • accepted 28 November 2014*)

Abstract−The feasibility of using rice husk for removing malachite green (MG) from aqueous solutions has been investigated as a low cost and an eco-friendly adsorbent. The effect of chemical treatment of rice husk by sodium carbonate was investigated through SEM and FTIR. As well, the effect of various factors like rotational speed, pH value of solution, temperature, initial concentration of dye, dose of adsorbent, contact time on the adsorption of MG was examined in batch experiments. Adsorption isotherms, kinetics, mass transfer and rate limiting steps are studied in detail. Adsorption thermodynamic parameters, activation energy and isosteric heat of adsorption were also studied. The adsorption was a spontaneous, endothermic and followed the pseudo-second-order kinetic model. The mechanism of adsorption and the COD aspect in deciding the effectiveness of the biomaterial as an adsorbent for dyes has also to be taken into account.

Keywords: Malachite Green, Adsorption Equilibrium, Kinetic, Thermodynamic Studies, SEM, FTIR, COD

INTRODUCTION

Malachite green (MG) is widely used synthetic and cationic dye. The molecular formula of malachite green is $C_{23}N_2H_{25}Cl$. Its molecular mass, melting point and color index number are 364.91 g mol^{-1}, 159 °C and 42000, respectively. MG is soluble in water and alcohol. It is stable, incompatible with strong oxidizing agents, strong acids, light-sensitive and combustible. When malachite green is dissolved in water the dye has a green color with an absorbance maximum at 617 nm. MG is extensively used as a dye in paper and pulp, leather, and textile industries. It is also widely used for various medicinal purposes, such as biological stain for microscopic analysis of cell biology and tissue samples.

Approximately 12% of synthetic dyes are lost during manufacturing and processing operations, and 20% of the resultant color enters the environment through effluents from industrial wastewater [1]. Like other dyes, MG is also very toxic and has the tendency to accumulate in the cells of living organisms and thus enters the food chain. It has extremely harmful consequences if it enters the eco system. Therefore, many countries have placed very stringent regulations and restrictions over the discharge of effluents from industries and also imports of items containing dye as a residue. As a result of strict enforcement of stringent regulation by the various environmental and governmental agencies upon the industries, there is a need to find cost-effective methods for removal of dyes from aqueous solution. The waste water containing dye(s) is difficult to treat since the dyes are very complex organic molecules, resistant to aerobic digestion and are stable to light, heat and oxidizing agents [2].

†To whom correspondence should be addressed.
E-mail: upendra_kumar72@rediffmail.com

During the past three decades, several physical, chemical and biological decolorization processes have been reported: coagulation, flocculation, biodegradation, adsorption on activated carbons, membrane separations, ion-exchange, oxidation, advanced oxidation process, biomass, selective biosorbents [3]. However, they have several disadvantages that include incomplete dye removal, high reagent and energy requirements and generation of toxic sludge or other waste products that requires proper disposal and further treatment. These methods are very costly, making them uneconomical and unviable [4]. Amongst the numerous techniques of dye removal, adsorption gives the best results [5]. Undoubtedly, activated carbon is the best known adsorbent [6], but its commercial use for the treatment of industrial effluents is restricted owing to its high cost and difficulty of regeneration from saturated state [7]. These limitations have forced researchers to look for alternative low cost and effective sorbents, which can be used as an alternative to the activated carbon. Researchers have recently investigated the different inexpensive and locally abundantly available biomaterials which are byproducts or the wastes from large scale industrial operations and agricultural waste materials like barley straw, waste tea leaves, sago waste, peanut hulls, hazel nut shell, saw dust, neem bark, chitin beads, thermally treated rice husk ash, waste banana, orange peels, cocoa shells, tree fern, coffee residue, palm kernel fiber, olive stone waste, grape stalk, bagasse, and fly ash as an adsorbent [8]. Using plant wastes as adsorbent for wastewater treatment is a simple technique that requires little processing, has good adsorption capacity, selective adsorption of heavy metal ions and dye, low cost, free availability, high efficiency, minimization of chemical or biological sludge, and easy regeneration.

Rice husk is a by-product of the rice milling industries which use paddy as a raw material. The paddy is produced in more than 75 countries, mostly belonging to developing countries. In the year 2010 a total of 678 million metric tons of rice was produced world-

wide [9]. As a rough estimate, rice husk consists of 20% of total paddy crops by weight. So roughly, 170 million metric tons of rice husk are produced worldwide per year. Disposal of rice husk is a great challenge and is generally disposed of, by burning in situ, producing significant amount of carbon dioxide and other harmful gases in the environment. Hence rice husk is easily and locally available in abundance at virtually no cost. It is chemically very stable, insoluble in water and possesses high mechanical strength. It also possesses a granular structure. Thus rice husk possesses all the desired characteristics of a good sorbent for water pollutants [9]. The various constituents and its composition are cellulose (25 to 35%), hemicelluloses (18 to 21%), lignin (26 to 31%), silica (15 to 17%), soluble (crude protein 2 to 5%) and moisture contents (7.5%) [10]. Although rice husk is an effective adsorbent for a wide range of solutes, particularly water pollutants, it suffers from at least two major drawbacks: low exchange or sorption capacity and poor physical stability (i.e., partial solubility) [11]. Therefore, to overcome the associated problems as stated above, it is necessary to modify the rice husk. As reported, three different techniques, namely mechanical (cutting, smashing, grinding etc.), physical (pyrolysis, combustion, burning, etc.) and chemical treatment with oxidizing agent such as ozone, hydrogen peroxide, acid (HCl, H_2SO_4, HNO_3, various organic acid etc), alkali (NaOH, KOH, NH_4OH etc) and salt solution (NaCl, Na_2CO_3) are available for the modification of rice husk.

In the present study, the effect of chemical treatment of rice husk by Na_2CO_3 was analyzed by SEM and FTIR study. Also, the effectiveness of sodium carbonate treated rice husk in removal of MG from aqueous solution was examined. An attempt was also made to understand the process of adsorption of MG onto SCRH through isotherm analysis, rate kinetic, thermodynamic analysis, etc., for the experimental data.

MATERIALS AND METHODS

1. Preparation of Adsorbent

The fresh rich husk was collected from a local rice mill and passed through different sieve sizes. The fraction of the particle between 425 and 600 micron (geometric mean size: 505 micron) was selected. The rice husk was washed thoroughly with distilled water several times to remove dirt and impurities. It was first air dried and then dried at temperature 60 °C. This was designated as raw rice husk (RRH). The dried rice husk was then suspended in 0.1 M sodium carbonate (Na_2CO_3) solution and kept in the shaker at temperature 40 °C and at 100 rpm rotational speed of the shaker for about 2 h. After 2 h, the shaker was switched off and it was left at normal temperature for next 24 h. The rice husk was filtered off and washed thoroughly with distilled water until the rice husk gave no color and the pH of the wash came close to neutral. The treated rice husk was then dried at 60 °C for 6 h. After drying, the adsorbent was stored in sealed glass containers and was designated as SCRH. SCRH was used in all the experiments.

2. Stock Solution

One gram of commercial grade malachite green was dissolved in one liter of distilled water to prepare the stock solution of 1,000 mg/L. Experimental dye solution of different concentrations was prepared by diluting the stock solution with suitable volume of distilled water.

3. Scanning Electron Microscope (SEM) Analysis

To characterize the surface structure and morphology of untreated, treated rice husk and treated rice husk after adsorption of MG, SEM analysis was carried out using a scanning electron microscope (Model JSM 6380 LA, JEOL Corp, Japan) at an electron acceleration voltage of 20 kV. Prior to scanning, the samples were coated with a thin layer of carbon using a sputter coater to avoid charging under the electron beam.

4. Fourier Transform Infrared Radiation (FTIR) Studies

The functional groups present in the rice husks were characterized by Fourier transform infrared radiation (FTIR) spectra. The FTIR spectra of both untreated and treated rice husk were obtained in transmission mode by using Affinity 1, Shimadzu Corp, Japan, spectrometer. The resolution of the spectrometer was kept 2 cm^{-1}. Samples were ground in ball mill and powders were pressed in KBr dishes to form the pallet sample. Each sample was exposed to 16 scans. The spectra range varied from 4,000 to 400 cm^{-1}.

5. Chemical Oxygen Demand (COD)

Chemical oxygen demand is a measure of the chemical (mostly organic) in the aqueous solution that consumes dissolved oxygen. COD is a useful measure of water quality. Many governments impose strict regulations regarding the maximum chemical oxygen demand allowed in wastewater before they can be returned to the environment. In the present study the COD of the distilled water, MG concentrations before and after the adsorption of MG with of 100 mg/L onto RRH and SCRH with an adsorbent dose 10 gm/L were measured in laboratory by redox titration method.

6. Batch Adsorption Experiments

The adsorption of MG on sodium carbonate treated rice husk was investigated in batch mode sorption experiments. All batch experiments were in 250 mL glass-stoppered Erlenmeyer flasks containing a fixed amount of adsorbent with 100 mL dye solution of known initial concentration. The flasks were agitated at a constant speed of 200 rpm for 90 min in an incubator shaker at predetermined temperature. The influence of pH (4.0, 5.0 6.0, 7.0, 8, 9), contact time (5, 10, 15, 20, 30, 45, 60, 90, 120 min), initial dye concentration (50, 100, 200 mg/L), and temperature (303 K, 313 K, 323 K) were evaluated during the present study. Samples were collected from the flasks at predetermined time intervals and investigated for the residual dye concentration in the solution by using double beam UV/VIS spectrophotometer Chemito (Model 3501/0706). The amount of dye adsorbed per unit adsorbent in mg/gm was calculated according to a mass balance on the dye concentration using Eq. (1).

$$q = \frac{(C_0 - C_t)V}{m} \quad (1)$$

All the experiments were performed twice and the average values of results were taken.

RESULTS AND DISCUSSION

1. Scanning Electron Microscope (SEM) Analysis

The SEM images of raw rice husk, sodium carbonate treated rice husk are shown in the Fig. 1(a) and (b). It is clear that both the raw

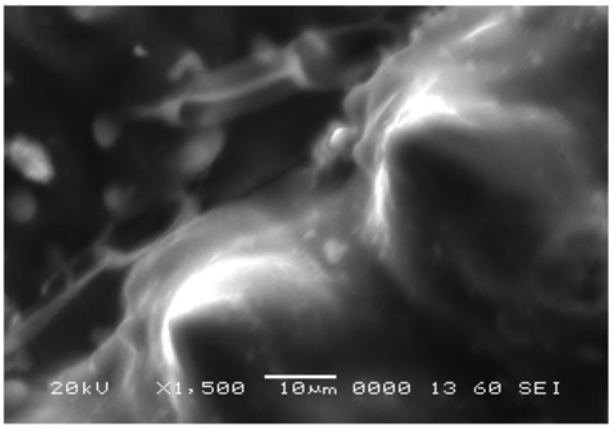

(a)

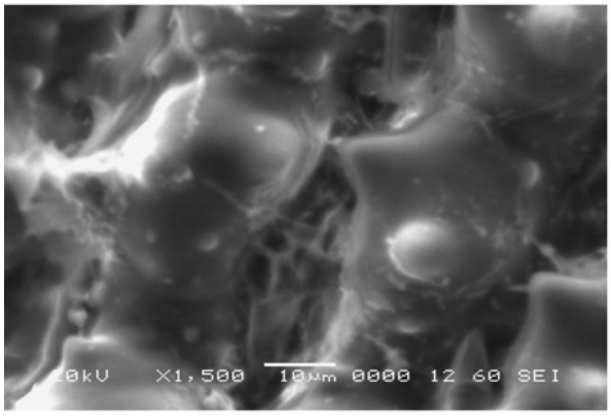

(b)

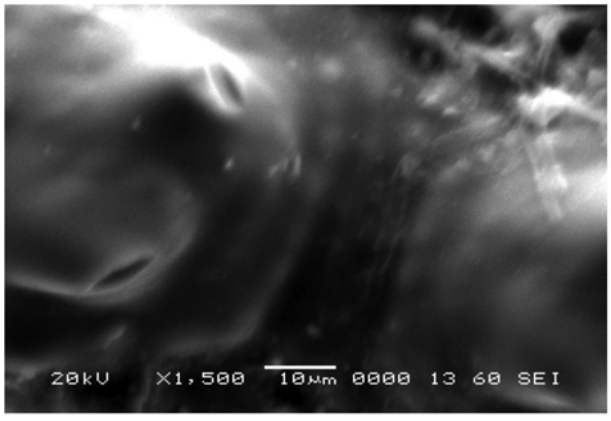

(c)

Fig. 1. SEM of (a) RRH (b) NCRH (c) NCRH after sorption.

rice husk and treated rice husk have an uneven, rough and porous surface which has a ridge type of pattern. The pores and cavities on the surface of both untreated and treated rice husk are heterogeneous, which provides a large exposed surface area for the adsorption. On comparing Fig. 1(a) and (b) it is evident that the surface morphology of raw rice husk changed significantly after treatment with sodium carbonate. More pores and cavities of various dimensions are clearly visible on the surface of treated rice husk in comparison to the raw rice husk. Prominent dome type structure can be seen at the SEM micrograph of raw rice husk. Most of the silica resides at the tip of the domes and their shoulders, whereas lower amount of silica is found elsewhere at the surface of the rice husk [12]. But such dome structure can be seen broken down for SCRH. This indicates at least a part of inorganic fraction mostly silica have been removed due to chemical treatment by Na_2CO_3. The Fig. 1(c) shows the micrograph of the sodium carbonate treated rice husk after the adsorption of malachite green. It can be observed that the micrograph is smooth and hardly any voids or pores are visible. This means that all the voids have been filled up by MG dyes during the process of adsorption.

2. Fourier Transforms Infrared Spectra (FTIR) Analysis

Fig. 2(a), (b) and (c) show the spectra of raw rice husk, sodium carbonate modified rice husk and potassium hydrogen phosphate treated rice husk, respectively. The FTIR spectra display a number of peaks, indicating the presence of several functional groups and complex nature of the rice husk. In the infra red absorption spectra of rice husk, the peak around the wave number 3,475.73 cm^{-1}, 3,437.15 cm^{-1} and 3,404.36 cm^{-1} represents the presence of hydroxyl group at the rice husk. There are two peaks at about 1,641.42 cm^{-1} that are the characteristic of carbonyl group C=O stretching hemicelluloses/wax. Besides, some characteristic peaks are observed at 1,413.82 cm^{-1} which indicates CH_2 strain, at 1,296.16 cm^{-1} representing CH bending, at 1,554.63 cm^{-1} indicating aromatic ring vibrations which can be only related to lignin. The inorganic part is characterized by group Si-O-Si at 1,083.99 cm^{-1}, Si-H (570.93, 536.21 cm^{-1}) [5,12]. It can be observed that the peak corresponds to the hydroxyl group in the spectra of sodium carbonate treated rice husk is sharper, has significant reduction in transmittance from 69% to 21% and shifted to wave number 3,444.87 cm^{-1}. This shows more exposure of the hydroxyl group after treatment of the rice husk by sodium carbonate. Instead of two peaks at about 1,641.42 cm^{-1} in the spectra of raw rice husk there is a single band with sharp peak at 1,641.42 cm^{-1} in the spectra of sodium carbonate treated rice husk. This decrease of peak and increase of sharpness of peak at 1,641.42 cm^{-1} may be due to partial elimination of waxes and/or hemicelluloses. Also, the spectra of sodium carbonate treated rice husk is more smooth, i.e., disappearance of many peaks in the hydroxyl band range in the spectra of sodium carbonate treated rice husk which are present in the spectra of raw rice husk indicates the removal of various impurities at the surface of the rice husk and the effectiveness of the chemical treatment. Fig. 2(c), which is the FTIR spectra of Na_2CO_3 treated rice husk after adsorption of malachite green, reveals that there is a shift in the peak of the band represents the hydroxyl group from wave number 3,444.87 cm^{-1} to wave number 3,437.15 cm^{-1} after the adsorption. Also the transmittance of this peak increases from about 21% to 54%. No appreciable changes either in shift in peaks or transmittance for the bands represented other functional group except hydroxyl group can be noticed in Fig. 2(c). This shows that mostly hydroxyl groups present at the surface of the treated rice husk are responsible for adsorption of MG.

3. Effect of Rotational Speed of the Shaker on Adsorption

Fig. 3 shows the effect of the rotational speed of shaker on the removal of dye from the solution. As the rpm increases the removal of dye increases up to 200 rpm, but further increase in speed caused a decrease in removal of dye from solution. It is because as rpm

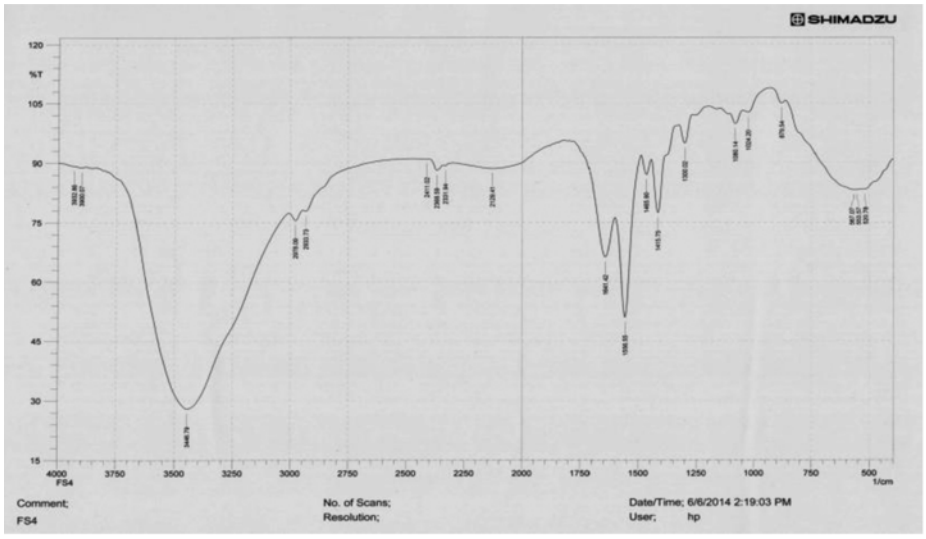

(a)

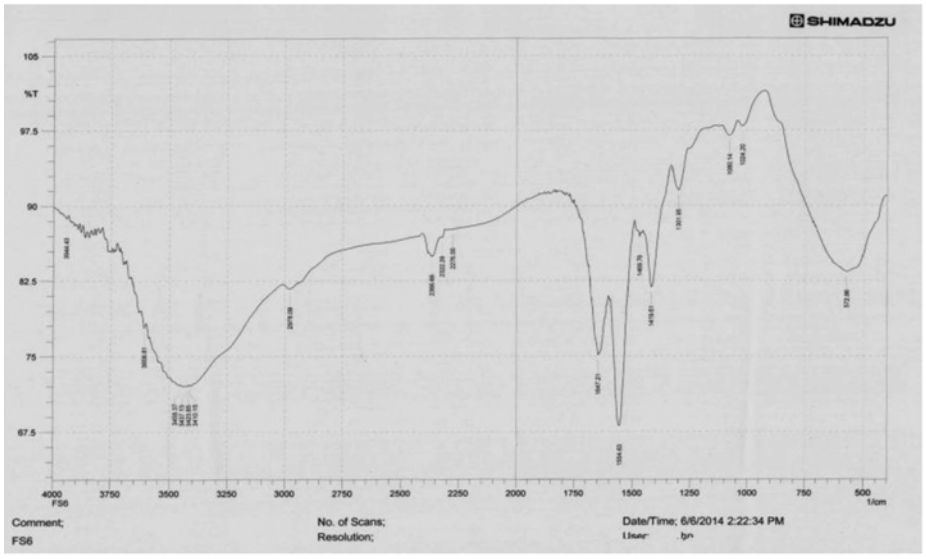

(b)

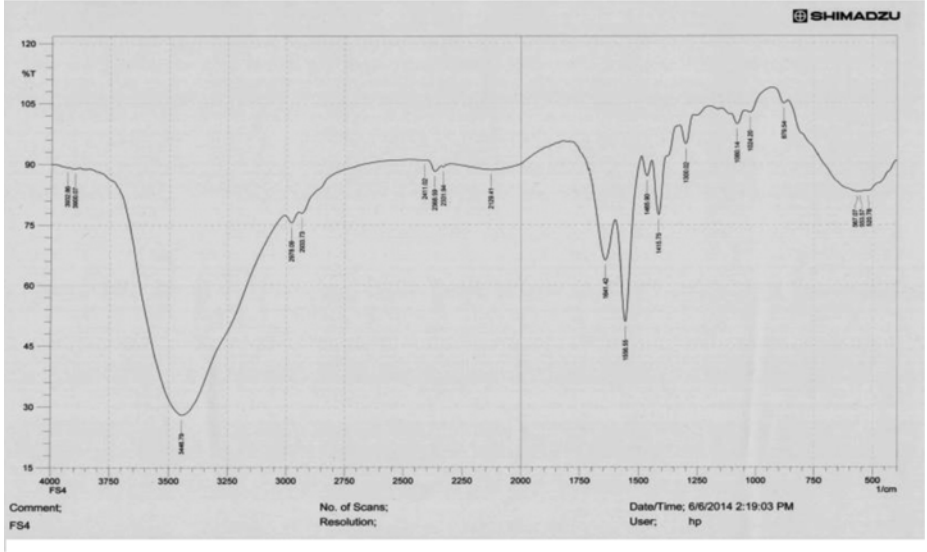

(c)

Fig. 2. FTIR Spectra of (a) RRH (b) NCRH (c) NCRH after sorption.

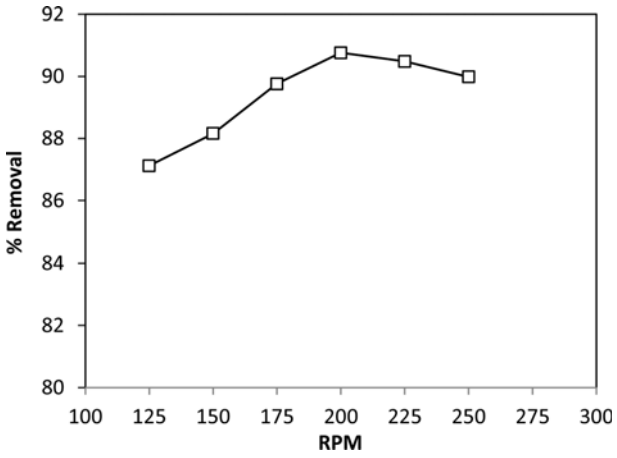

Fig. 3. Effect of rotational speed on removal of malachite green.

increases, the migration of dye molecules from solution to the surface of adsorbent increases. Also, because of rotational speed the dye molecules acquire more kinetic energy, and hence the effect of boundary layer gets reduced. Thus, adsorption increases on increasing rotational speed of the shaker. The reduction in removal of dye at rpm more than 200 may be explained from the fact that, due to rotational motion, a centripetal force which is given by relation $m\omega^2 r$ acts on the adsorbed dye molecule and adsorbent differently because of their difference in mass. So they have a tendency to readjust the radius of their path. As a result, they feel a repulsive force between them. The magnitude of separative force, which depends upon rpm, increases with increase in rotational speed and becomes greater than the binding force when rpm exceeds 200. Hence, at higher speed desorption increases, and as a result the removal of dye from solution decreases.

4. Effect of pH

Fig. 4 shows the effect of pH on the removal efficiency of MG which was studied at different pH ranging from 4.0 to 9.0. The equilibrium uptake of MG increased notedly with raising the pH from 4.0 to 6.0. Above these levels, the adsorption capacity did not change significantly up to pH 9.0. Similar trend was reported for adsorption of MG on rubber wood (*Hevea Brasiliensis*) sawdust [13] treated ginger waste [3], maize cob powder [14]. The maximum sorption capacity takes place between pH 7 to 7.5. Therefore, further experiments were performed at pH 7-7.5. MG is a cationic dye, so the surface charge density over the surface of the SCRH which is affected by the pH value of the solution, greatly influences the adsorption of MG. At low pH, i.e., in excess of H^+ ions, the probability of the protonation of the functional group present at the surface of the adsorbent increases, thereby restricting the positively charged dye cations to adhere at the surface of the adsorbent. As pH increases, the availability of proton in solution decreases and hence protonation of functional group decreases, resulting in an increase in the negative charge density on the adsorbent surface and facilitate the binding of cationic dye by electrostatic attraction. In simple words, the increase in dye removal capacity at higher pH up to 7 attributes to the reduction of H^+ ions which compete with cationic dye for appropriate sites on the adsorbent surface. But at higher pH (>7), there is an excess of OH^- ions present in the solution which compete with negatively charged SCRH in attracting the cationic MG dye molecules. Thus removal decreases at pH greater than 7.

5. Effect of Contact Time

From Fig. 5, the adsorption of MG took place rapidly up to 30 min there after it slowed and attained equilibrium about 90 min. Further increase in contact time does not enhance the adsorption. Initially, the rate of adsorption was rapid due to the adsorption of dye molecules onto the exterior surface. After that the molecules enter into pores (interior surface), a relatively slow process. The initial faster rates of adsorption may also be attributed to the presence of large number of binding sites for adsorption and the slower adsorption rates at the end is due to the saturation of the binding sites and attainment of equilibrium. Similar conclusions have been proposed by Linh et al. (2012) for adsorption of MG onto rubber wood (*Hevea Brasiliensis*) sawdust [13]. The adsorption reached equilibrium within 90 min and was independent of the initial dye concentration.

6. Effect of Adsorbent Dose

Fig. 6 shows the influence of adsorbent dose on the rate of adsorption of MG onto SCRH. The experiment was carried out with

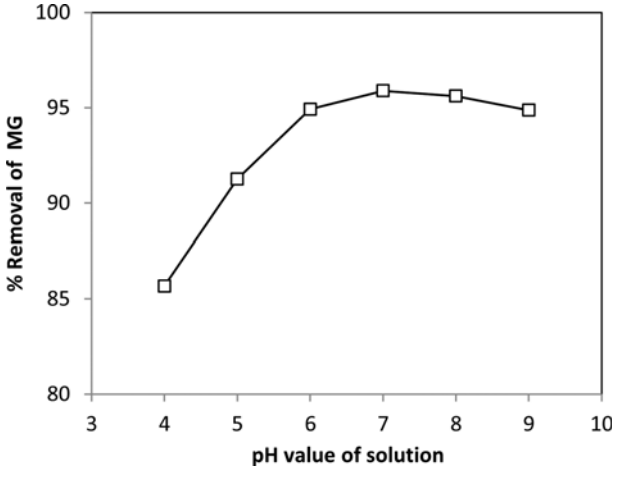

Fig. 4. Effect of pH on removal of malachite green.

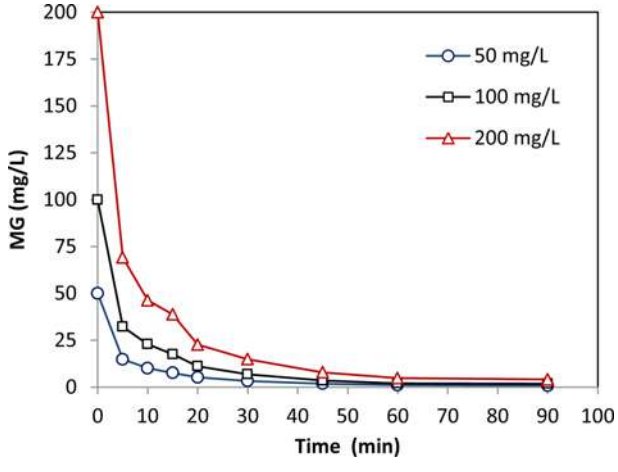

Fig. 5. Effect of contact time and initial concentration of malachite green.

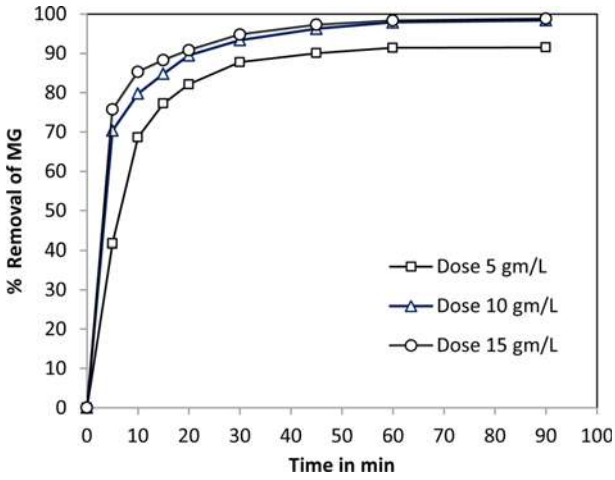

Fig. 6. Effect of adsorbent dose on removal of malachite green.

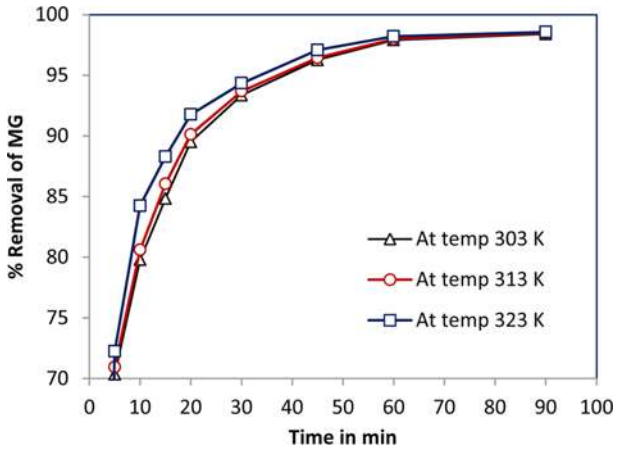

Fig. 7. Effect of temperature on removal of malachite green.

fixed initial concentration of 50 mg/L of MG, temperature at 30 °C, at basic pH condition and at three different dose of 5, 10, 15 gm/L of SCRH. It was observed that percentage of dye removal increased with increase of adsorbent dose. Such a trend is mostly attributed to an increase in the adsorptive surface area and the availability of more active adsorption sites [15]. Whereas, the sorption capacity, which is defined as the ratio of the amount of adsorbate in mg adsorbed to the amount of adsorbent in gm, decreased with increase in dose. Adsorption capacity of SCRH at equilibrium were found to be 9.152, 4.92 and 3.29 mg/gm respectively for dose of 5, 10. 15 gm/L. There was marginal decrease in the sorption capacity at equilibrium for doses of 10 and 15 gm/L This may be attributed to overlapping or aggregation of adsorption sites, resulting in a decrease in total adsorbent surface area available to MG and as an increase in diffusion path length, and hence, the sorbent dose of 10 gm/L of SCRH seems to be optimal and was selected for the further detailed kinetic study.

7. Effect of Initial Concentration

Fig. 5 shows the influence of the initial concentration of MG in solution on the rate of adsorption. The experiment was carried out with fixed adsorbent dosage 10 gm/L, temperature at 30 °C and at basic pH condition. The percent adsorption decreased from 98.8% to 98.08% with an increase in initial dye concentration from 50 mg/L to 200 mg/L. Similar observation of small decrease in percentage removal of dye with increase in initial MG concentration was noticed by Kumar et al. [2]. This is because after the formation of mono layer at the lower initial concentration of dye over the surface of adsorbent any further formation of layer of dye species is highly hindered. The adsorption capacity for SCRH increased from 4.94 to 19.62 mg/g at equilibrium as the MG concentration in the test solution was increased from 50 to 200 mg/L Increasing the initial dye concentration results in an increase in the adsorption capacity because it provides a driving force due to higher concentration gradient between aqueous and solid phase to overcome all mass transfer resistances of dyes between the two phase.

8. Effect of Temperature

Fig. 7 shows the rate of adsorption of MG onto SCRH which was investigated at temperature 303 K, 313 K, 323 K with initial dye concentration of 50 mg/L and dose of 10 gm/L. It can be seen that the adsorption of dye increased with increase in temperature, which indicates that a high temperature favored MG removal by adsorption onto SCRH. This may be attributed to increase in the number of active surface sites available for adsorption, increase in the porosity and in the pore volume of the adsorbent. The viscosity of fluid decreases with increase in temperature. This leads to increases in the rate of diffusion of adsorbate molecules across the external boundary layer and within the internal pores of the adsorbent particles. The kinetic energy, i.e., the mobility of molecule increases with increase in temperature. This may also result in enhancement in adsorption. The finding is in agreement with the observations of Daneshvar et al. [16] on the bio sorption of MG on Cosmarium species [16]. The increase of the equilibrium uptake with increase in temperature means that the dye adsorption process is an endothermic process.

9. Adsorption Isotherms

In the present study four isotherm models, namely, Freundlich, Langmuir, Temkin and Dubinin-Radushkevich (D-R), were fitted with the experimental equilibrium data for adsorption of MG onto SCRH at different temperatures. These isotherm models in linear form are represented by the Eqs. (1), (2), (3) and (4) in Table 1. The results are shown in Table 2.

The value of b, the Langmuir isotherm constants, Freundlich constants and B_B the Temkin constant increased with increase in temperature, which accounts for the endothermic nature of the adsorption process. The value of R_L lies between 0 and 1, which suggests the favorable nature of the adsorption process. The values of n ($2<n<10$) represent a favorable sorption. The value of E obtained from D-R model was higher than 8 kJ/mol at temperature 313 K and 323 K and it was nearly equal to 8 kJ/mol at temperature 303 K, indicating that the adsorption mechanism was chemical sorption. The correlation coefficients (R^2) of the four isotherms are also listed in Table 2. On comparing the correlation coefficient values, it could be concluded that the adsorption of MG onto SCRH best fitted to the Langmuir isotherm model under the temperature range studied. However, the value of R^2 for Freundlich and Temkin model are 0.938, 0.941, 0.938 & 0981, 0.984, 0.983 at temperature 303 K, 313 K, 323 K, respectively. These values are quite high and nearer

Table 1. Compilation of different model in linear form used in the study

Model/equation	Equation	Remarks (description of various quantities)
1. Langmuir isotherm model	$\frac{1}{q_e}=\left(\frac{1}{Q_0 b}\right)\left(\frac{1}{C_e}\right)+\frac{1}{Q_0}$	V=total volume of solution (L) m=mass of the adsorbent in the solution (gm) q=amount of adsorbate adsorbed at the time t (mg/gm) q_e=amount of adsorbate adsorbed at equilibrium (mg/gm) Q_0=maximum adsorption capacity (mg/gm) for forming single layer C_0=initial adsorbate (dye) concentration in (mg/L) C_e=equilibrium concentration of dye in (mg/L) b=Langmuir isotherm constant in (mg/L) K_F=Freundlich's adsorption capacity (mg/gm) n=adsorption intensity constants q_S=theoretical isotherm saturation capacity (mg/g), β=Dubinin-Radushkevich isotherm constant ($mmol^2/J^2$) E=mean sorption energy K_T=Temkin adsorption potential in (L/g) B_T=Temkin constant K_{p1}=the pseudo first order rate constan K_{p2}=pseudo second order rate constant K_{id}=intraparticle rate constant C_i=Thickness of the boundary layer $F=q_t/q_e$=fractional attainment of equilibrium
Dimensionless separation factor	$R_L=\frac{1}{(1+bC_0)}$	
2. Freundlich isotherm model	$\ln q_e=\ln K_F+\frac{1}{n}\ln C_e$	
3. Dubinin-Radushkevich isotherm model	$\ln q_e=\ln q_S-\beta\varepsilon^2$ where $\varepsilon=RT\ln(1+1/C_e)$ and $E=(1/2\beta)^{1/2}$	
4. Temkin Isotherm model	$q_e=B_T\ln K_T+B_T\ln C_e$	
5. Pseudo first order rate model	$\ln(q_e-q)=-K_{p1}t+\ln q_e$	
6. Pseudo 2nd order rate model	$\frac{t}{q}=\frac{t}{q_e}+\frac{1}{K_{p2}q_e^2}$	
7. Weber & Morris model	$q_t=K_{id}t^{1/2}+C_i$	
8. Liquid film diffusion model	$\ln(1-F)=-k_{fd}t$	

Table 2. Adsorption isotherm parameters of MG

Isotherm model	Parameter	Temperature in Kelvin		
		303 K	313 K	323 K
Langmuir model	Q_{max} (mg/gm)	25.64	26.32	27.03
	b (L/mg)	0.339	0.362	0.377
	R_L	0.029	0.027	0.026
	R^2	0.997	0.993	0.996
Freundlich model	K_F (mg/gm)	9.631	9.924	10.16
	n	4.03	4.04	4.01
	R^2	0.938	0.941	0.938
Temkin model	K_T (L/mg)	6.92	7.51	7.78
	B_T	4.243	4.283	4.385
	R^2	0.981	0.984	0.983
Dubinin-Radustrkevich model	q_s (mg/gm)	21.63	22.18	22.53
	β (m-mole^2/j^2)	8×10^{-9}	7×10^{-9}	5×10^{-9}
	E (kj/mole)	7.91	8.45	10.00
	R^2	0.887	0.904	0.894

C_o=100 mg/L, pH-7, rpm - 200, dose 1 to 10 gm/L

to 1; hence it may be considered that the adsorption of MG onto SCRH also follows both the Freundlich and Temkin model.

10. Adsorption Kinetics

In the present study the pseudo-first-order rate equation and the pseudo-second-order rate equation in linearized form (Eqs. (5) and (6) in Table 1) were fitted to the experimental data at different concentrations and temperatures [17,18]. Results are shown in Table 3 and Table 4. Based on the value of R^2 it is concluded that the adsorption of MG onto SCRH best fitted with pseudo-second-order rate model. The small difference between the $q_{e,\,exp}$ and $q_{e,\,cal}$ for pseudo-second-order rate model is further reinforcing the applicability of the pseudo-second-order model. Table 4 shows that rate constant, K_{p2} increases as the temperature increases, indicating endothermic nature of adsorption of MG onto SCRH. Similar results were previously reported for adsorption of MG onto chlorella-based biomass [19].

11. Mass Transfer Parameter and Rate Limiting Step

The pore or intraparticle diffusion, the rate limiting step is determined by the equation proposed by Weber & Morris [17,18] as shown by Eq. (7) in Table 1. The result is shown in Fig. 8. It is evident that the whole part of the curve consists of three straight lines.

Table 3. Adsorption kinetic parameters at various initial concentration of MG

C_0 (mg/L)	$q_{e,\,exp}$ (mg/gm)	Pseudo second order			Pseudo first order		
		$q_{e,\,Cal}$ (mg/gm)	K_{P2}	R^2	$q_{e,\,Cal}$ (mg/gm)	K_{P1}	R^2
50	4.92	5.076	0.0765	0.999	2.59	0.077	0.962
100	9.815	10.20	0.0338	0.999	6.81	0.094	0.971
200	19.592	20.40	0.0157	0.999	12.49	0.84	0.978

Temp.=30 °C, rpm=200, pH=7, dose=10 gm/L

Table 4. Adsorption kinetic parameters at various temperature of MG

Temperature (K)	$q_{e,\ exp}$ (mg/gm)	Pseudo second order			Pseudo first order		
		$q_{e,\ Cal}$ (mg/gm)	K_{P2}	R^2	$q_{e,\ Cal}$ (mg/gm)	K_{P1}	R^2
303	4.92	5.076	0.0765	0.999	2.59	0.077	0.962
313	4.925	5.076	0.0812	0.999	2.47	0.076	0.958
323	4.928	5.05	0.099	1.000	2.31	0.081	0.955

Co=50 mg/L, dose=10 mg/L, rpm=200, pH=7

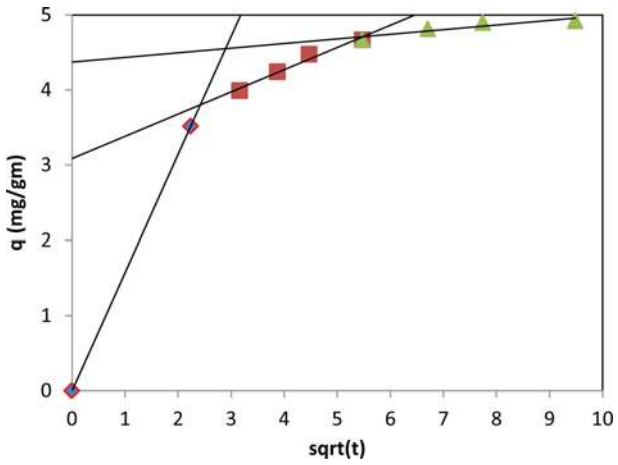

Fig. 8. Test plot for the Weber & Morris model.

Initially, the line passed through the origin, but as time passed there was an increase of intercept, i.e., the thickness of the boundary layer increased with time. As the plots did not have a zero intercept, it may be concluded that film diffusion and intraparticle diffusion were concurrently operating during interaction of MG with sodium carbonate treated rice husk. The diffusion of the adsorbate from the bulk liquid phase to the surface of the adsorbent might also play an important role in determining the rate of an adsorption process. Therefore, the kinetic data were analyzed by the liquid film diffusion model as shown by Eq. (8) in Table 1. The plots of ln(1−F) versus t are shown in Fig. 9. The linear plots did not pass through the origin, suggesting limited applicability of the liquid film diffusion model in the present adsorption system.

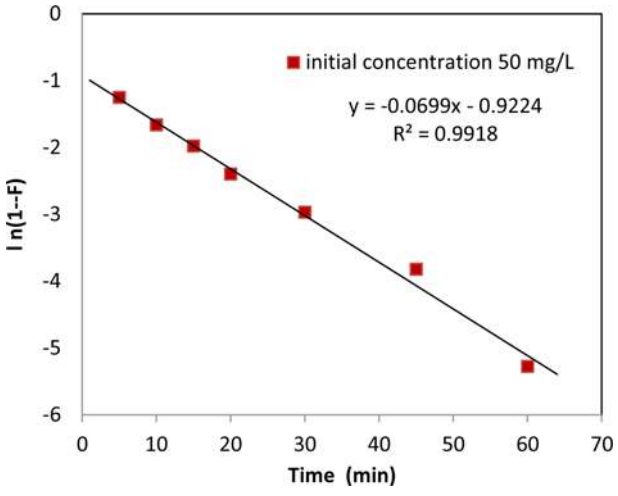

Fig. 9. Test plot for the Liquid film diffusion model.

12. Activation Energy

Adsorption of adsorbate particle (molecule, atom or ions) onto the surface of adsorbent takes place only when the adsorbate particle collides with the surface of adsorbent having certain minimum energy and a definite orientation. It appears that there is an energy wall at the surface and the adsorbate particle has to cross this wall for adsorption onto the surface of adsorbent. This minimum energy which is required for the adsorbate particle to get adsorbed at the surface of adsorbent is known as activation energy. Arrhenius has given an empirical relation which is represented in linear form as

$$\ln K = \ln A - \frac{E_a}{RT} \tag{9}$$

K is the rate constant of adsorption. In the present case it is the pseudo-second-order rate constant (K_{p2}). R is ideal gas constant; A is the proportionality constant which varies from one process to another. E_a is the activation energy of the process and T is temperature in Kelvin. The value of E_a is calculated from slope of the straight line plotted between $\ln K_{p2}$ versus 1/T which in present case is 10.28 KJ/mole. According to literature, if activation energy of the process is between 8.4 and 83.7 KJ/mole, then the process may be an activated chemical adsorption process, which is the present case [20].

13. Thermodynamic Parameters

The thermodynamic parameters such as standard state Gibbs free energy change (ΔG^0), standard state enthalpy change (ΔH^0) and change in standard state entropy (ΔS^0) were calculated using the van't Hoff equation [20].

$$\Delta G^0 = -RT \ln K \tag{9}$$

$$\Delta G^0 = \Delta H^0 - T\Delta S^0 \tag{10}$$

where K is the equilibrium constant of adsorption process, considering it as a chemical reaction between adsorbate molecule and the active site at the adsorbent. Since adsorption of MG onto SCRH follows pseudo-second-order rate reaction. So according to the underlying presumption for the pseudo-second-order rate reaction, the rate of reaction at any instant depends upon the concentration of the MG and independent of the active sites [21]. The reaction may be represented as

$$2A + S_v = AS$$

where A is the MG molecule, S_v is the available vacant site at the surface of the SCRH and AS is the adsorbed MG onto SCRH surface.

Rate of forward reaction=$K[A]^2\cdot[S_v]=K^+[A]^2$; where $K^+=K[S_v]$
Rate of backward reaction=$K^-[AS]$
At equilibrium,
Rate of forward reaction=Rate of backward reaction

The equilibrium constant is defined as

$$K=\frac{K^+}{K^-}=\frac{[AS]}{[A]^2}$$

If C_0 is the initial concentration and C_e is the concentration at equilibrium then at equilibrium $[A]=C_e$ and $[AS]=C_0-C_e$ and

$$K=\frac{C_0-C_e}{C_e^2} \quad (11)$$

According to the abundant available literature, various researchers have taken different value of K for calculation of ΔG^0, ΔH^0 and ΔS^0. Chowdhury et al. [22] took $K=C_0/C_e$, Xin et al. [10] have taken three empirical values of K ($K=1/b$, $K=K_F^n$ and, $K=q_e/C_e$), Subbareddy et al. [23] took K=b for calculation of these parameters. In the present analysis the value of ΔG^0 was calculated from Eq. (11) and Eq. (9), and then by plotting the straight line as per Eq. (10) between T versus ΔG^0, the value of ΔH^0 and ΔS^0 were calculated from the intercept and slope of the straight line. The results are shown in Table 5. The negative value of ΔG^0 at all temperature shows that the process is favorable and spontaneous. The positive value of ΔH^0 is indicating that the process is endothermic and the positive value of ΔS^0 showing increases in randomness at the surface of adsorbent and the adsorption process involves a dissociative mechanism; it is in perfect agreement with the second law of thermodynamics. Further, from the plot the governing Eq. (10) comes out to be $\Delta G^0=-0.064\,T+8.621$.

For adsorption to take place ΔG^0 must be less than 0: $-0.064\,T+8.621<0$. This implies that T>134.7 K. Hence from thermodynamic analysis the adsorption of MG onto NCRH is feasible at all temperature above 134.7 K. Table 5 shows that the value of ΔG^0 decreases with increase in temperature. It suggests that the adsorption is favorable at higher temperature. This was what exactly was being observed during experiment. The reason might be that mobility of adsorbate ions/molecules in the solution increased with increase in temperature and that the affinity of adsorbate on the adsorbent is higher at high temperatures. Oepen et al. [24] detected the sorption free energy of several kinds of interactions [24]. According to them for van der Waals force sorption free energy is 4-10 kJ/mol, for hydrophobic force it is about 5 kJ/mol, for hydrogen bond it is 2-40 kJ/mol, for coordination exchange it is 40 kJ/mol, for dipole force it is 2-29 kJ/mol, and for chemical bond it is above 60 kJ/mol [10]. From the value of ΔH^0 which is shown in Table 5 it can be concluded that the main interactions between cationic MG and sodium carbonate treated rice husk (SCRH) are probably hydrogen bond and/or dipole force.

Table 5. Adsorption thermodynamic parameters of MG

Temperature (K)	ΔG^o (KJ/mole)	ΔH^o (KJ/mole)	ΔS^o (J/mole)	R^2
303	−10.9386	8.621	64	0.997
313	−11.6381			
323	−12.2308			

C_o=50 mg/L, dose=10 gm/L, pH- 7, rpm - 200

14. Isosteric Heat of Adsorption

The isosteric heat of adsorption is defined as the heat of adsorption at constant surface coverage, i.e., at constant amount of adsorbate adsorbed. It is calculated using the Clausius-Clapeyron equation:

$$\ln C_e=\left(\frac{\Delta H_x}{R}\right)\frac{1}{T}+\text{constant} \quad (12)$$

where, C_e is the equilibrium adsorbate concentration in the solution (mg/L), ΔH_x is the isosteric heat of adsorption (kJ/mol), R is the ideal gas constant (8.314 J/mol/K), and T is temperature. Eq. (12) is in the form of straight line and known as adsorption isostere. The slope of the straight line between C_e vs 1/T gives the value of (H_x/R). The value of C_e for constant surface loading is obtained from the best fitted isotherm model, which is the Langmuir isotherm model at 303 K, 313 K and 323 K, respectively. Result is shown in Fig. 10 and Table 6. Isosteric heat of adsorption of MG onto SCRH is positive, which confirms the endothermic nature of adsorption process. It also shows that ΔH_x increases with increase in surface loading, indicating the presence of energetically heterogeneous surfaces of adsorbent. Otherwise for homogeneous surface, it would be constant. Adsorbate-adsorbate interaction followed by adsorbate-adsorbent interaction might be the reason for dependence of ΔH_x on the surface loading. Initially adsorbate-adsorbate interaction takes place at lower q_e values resulting in low ΔH_x values. With increase in q_e, adsorbate-adsorbent interaction dominates, resulting in high value of ΔH_x. The increase in isosteric heat with increase in surface coverage was also indicative of the presence of strong lateral interaction between adsorbed molecules [6,25].

15. Adsorption Mechanism

According to the experimental findings and analysis of the present study, the following observations have been made:

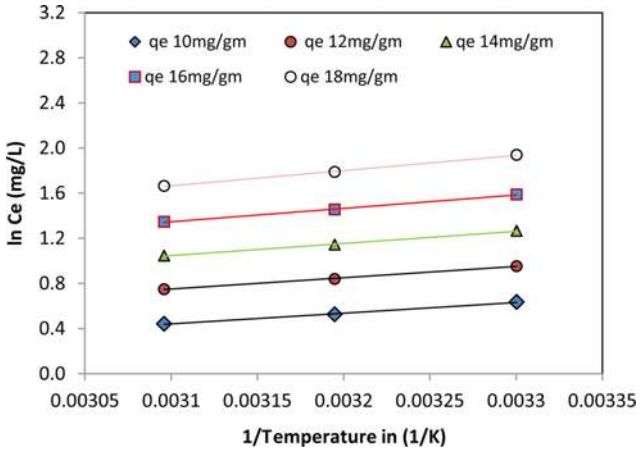

Fig. 10. Test plots for Clausius-Clapeyron.

Table 6. Isosteric heat of adsorption of MG

Surface loading (mg/gm)	10	12	14	16	18
Isosteric heat (kJ/mole)	7.82	8.30	8.94	9.83	11.14

1) Adsorption of MG onto SCRH was very rapid, initially up to first 30 min and afterward slowed down. More than 90% removal was observed at 30 min. It reached equilibrium in about 90 min. Adsorption was highly pH dependent and optimum pH was observed as 7.

2) The adsorption of MG onto the SCRH followed the pseudo-second-order rate kinetic equation, which suggests that two molecules of MG adhere to one active site at the surface of the SCRH.

3) Only those MG molecules get adsorbed which migrate to the surface of SCRH with energy greater than the activation energy and with proper orientation. Others will not get adsorbed.

4) The main interactions between cationic MG and sodium carbonate treated rice husk (SCRH) are probably hydrogen bond and/or dipole force.

Based on these observations and on the structure of the adsorbate and adsorbent surface properties, the mechanism for the re-

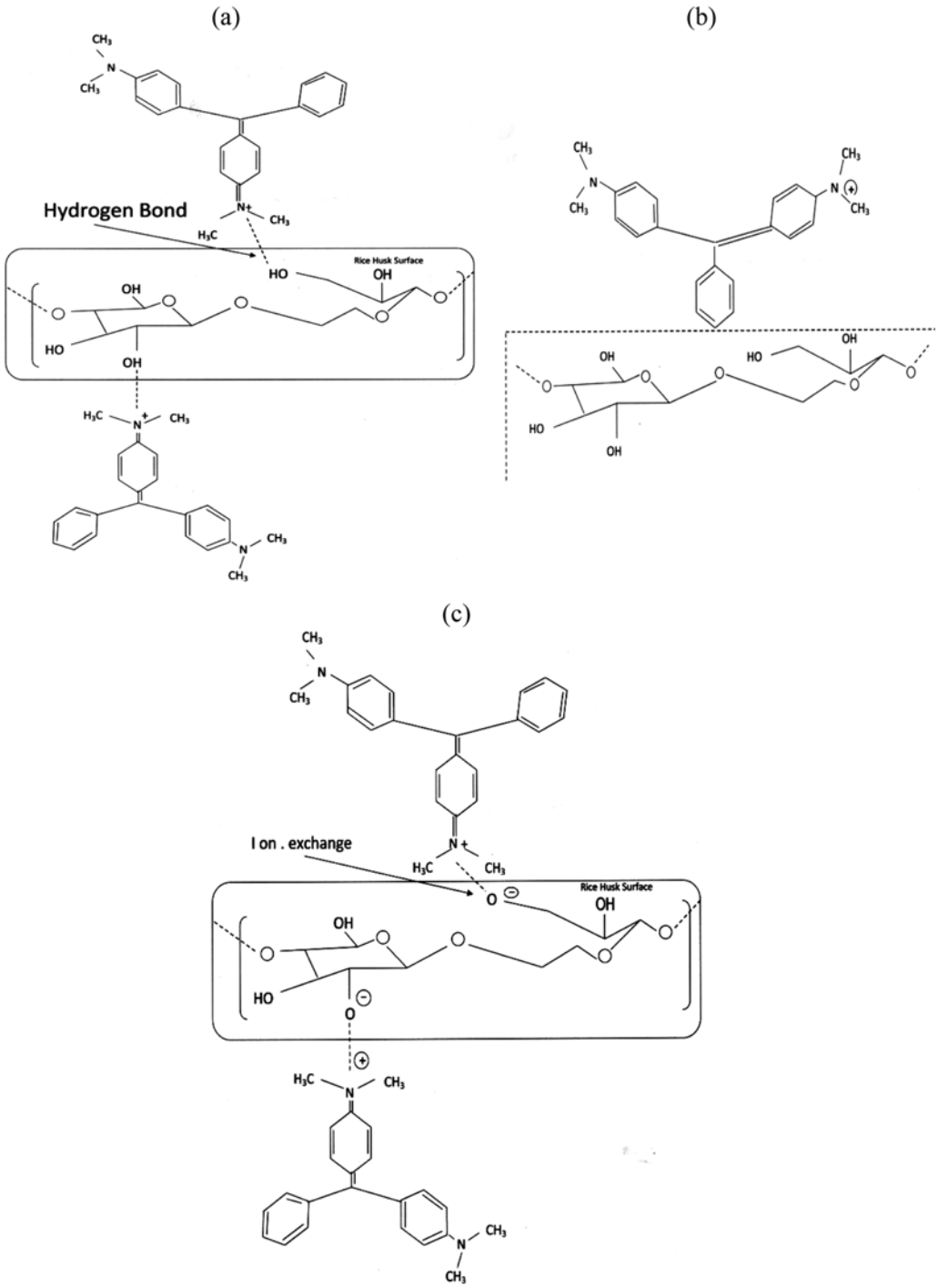

Fig. 11. Representation of (a) surface hydrogen bonds between the hydroxyl groups on the SCRH surface and the nitrogen atoms of MG (b) another possibility of approaching the MG molecule at the surface of the SCRH (c) ion-exchange mechanism.

moval of MG by adsorption on sodium carbonate treated rice husk may be assumed to involve the following steps:

- Migration of dye from bulk of the solution to the surface of the adsorbent under the influence of concentration gradient and due to externally induced agitation by shaker.
- Diffusion of dye through the boundary layer to the surface of the adsorbent.
- Adsorption of dye on the surface of treated rice husk. Adsorption of MG onto SCRH was very rapid; initially up to first 30 min more than 90% removal was observed. So it is clear that the major adsorption takes place in the surface of treated rice husk. This film diffusion plays an important role in the present case.

Adsorption of dye on the surface of treated rice husk may be due to the formation of surface hydrogen bonds between the hydroxyl groups on the rice husk surface and the nitrogen atoms of MG as suggested in Fig. 11(a).

Fig. 11(b) shows another possibility of approaching the MG molecule at the surface of the SCRH, but it does not get adsorbed because it is not approaching with proper orientation. From Fig. 11(b) it is clear that the distance between N atom of MG molecule and H atom of hydroxyl group at the surface of SCRH is too large to form a hydrogen bond.

Further study and experiment is required to determine experimentally the heat of adsorption of MG onto SCRH, the bond length and bond angle before reaching at final conclusion.

Another mechanism of a dye-hydrogen ion exchange may be taken into consideration as:

$$C_{23}N_2H_{25}Cl \rightarrow C_{23}N_2H_{25}^{+} + Cl^{-}$$
$$R\text{-}(OH)_2 \rightarrow R\text{-}O_2^{-2} + 2\,H^{+}$$
$$2C_{23}N_2H_{25}^{+} + R\text{-}O_2^{-2} \rightarrow RO_2(C_{23}N_2H_{25})_2$$

MG is represented by $C_{23}N_2H_{25}Cl$. The cellulose and hemicellulose of the sodium carbonated rice husk is represented as R-$(OH)_2$. Ion exchange can be one of the possible mechanisms, then the pH of the effluent gets decreased due to presence of excess H^+ ion in the residual solution as shown in the above equation. However, during experiment no appreciable decrease in pH was noticed. So it is clear that ion exchange mechanism is not involved. The value of ΔH^0 (8.621 KJ/mole) also ruled out ion exchange mechanism. According to Lyubchik et al. [26] the enthalpy changes for ion-exchange reactions are usually smaller than 8.4 kJ/mol [26].

- Intra particle diffusion of dye into the interior pores of the adsorbent. As reported earlier by using the Weber & Morris model, the plots did not have a zero intercept, so it may be concluded that film diffusion and intra particle diffusion were concurrently operating during interaction of MG with sodium carbonate treated rice husk and intra particle diffusion was not the major phenomenon of adsorption.

Desorption experiment was also performed with the MG adsorbed SCRH at 200 rpm for 1 h in the normal tap water at neutral pH and at 30 °C. It was observed that MG could not get desorbed. So it is clear the MG has adsorbed onto SCRH by strong bond, which may be due to the formation of surface hydrogen bonds between the hydroxyl groups on the rice husk surface and the nitrogen atoms of MG, as suggested in Fig. 11(a).

From all the above conclusions, it is clear that the mechanism of adsorption is due to the formation of surface hydrogen bonds between the hydroxyl groups on the rice husk surface and the nitrogen atoms of MG. Film diffusion and intra particle diffusion were concurrently operating during interaction of MG with sodium carbonate treated rice husk and film diffusion was not the major phenomena of adsorption.

16. Chemical Oxygen Demand Analysis

The initial COD concentration of MG solution was observed as 86.64 mg/L, which reduced to 50.86 mg/L when treated with SCRH and the COD concentration increased to 116.52 mg/L when treated with RRH at 10 gm/L for 90 min, respectively. This decrease of COD was not in proportion to the decrease in the concentration of MG from the solution. The reason may be that the rice husk adsorbed MG also left some organic matter into the solution, which ultimately contributed to the COD of the treated solution. Further, it can be seen that the COD of solution after adsorption of MG onto RRH increased from the initial COD of the MG solution. The improvement in the performance of the SCRH compared to the RRH on this count may be due to the fact that percentage removal of MG from solution was much higher by SCRH than by RRH. Since RRH increases the COD of the initial solution, hence it cannot be used for removal of dyes from waste water. Also, there is the possibility that the organic substances which were otherwise left behind in the solution were washed off during chemical modification of rice husk by sodium carbonate. Hence for effective biosorbents it should effectively removes dyes from waste water as well as reduce the COD to the permissible limit.

CONCLUSION

Sodium treated rice husk can be used for removal of malachite green from aqueous solution up to 98%, depending upon the initial concentration. The optimum pH, rpm, adsorbent dose and maximum adsorption capacity were 7.0, 200, 10 g/L and 25.88 mg/gm, respectively. The adsorption capacity increased with the rise in temperature, indicating that the adsorption was a spontaneous, endothermic process. The adsorption data showed good agreement with the pseudo-second-order kinetic model for different sorbent concentration and temperature. The process was endothermic. The negative value of ΔG^0 indicates that the adsorption process was spontaneous and favorable, the positive value of ΔH^0 is indicating that the process was endothermic, and the positive value of ΔS^0 showing increases in randomness at the surface of adsorbent and the adsorption process involved a dissociative mechanism. The COD measurement suggests that in concluding that a particular biosorbent is good alternative to activated carbon, a COD analysis should also be done. Finally, sodium carbonate treated rice husk can be an economical alternative material to more costly adsorbents like activated carbon used for removal of malachite green in wastewater treatment processes.

ACKNOWLEDGEMENTS

The authors greatly appreciate the World Bank TEQIP II fund of MHRD, Govt. of India for the financial support. The authors are also grateful to all the Civil and Environmental Engineering

teams of the National Institute of Technology, Silchar, Assam, India, for their support and encouragement.

REFERENCES

1. X. Q. Yang, X. X. Zhao, C. Y. Liu, Y. Zheng and S. J. Qian, *Process Biochem.*, **44**(10), 1185 (2009).
2. P. S. Kumar, S. Ramalingam, C. Senthamarai, M. Niranjanaa, P. Vijayalakshmi and S. Sivanesan, *Desalination*, **261**(1-2), 52 (2010).
3. R. Ahmad and R. Kumar, *J. Environ. Manage.*, **91**(4), 1032 (2010).
4. S. M. Ghoreishi and R. Haghighi, *Chem. Eng. J.*, **95**, 163 (2003).
5. D. Rosa, I. M. Kenny, J. M. Pugkia, D. C. Santulli and F. Sarasini, *Compos. Sci. Technol.*, **70**, 116 (2010).
6. F. Derbyshire, M. Jagtoyen, R. Andrews, A. Rao, I. Martin-Gullon and E. Grulke, *In Chemistry and Physics of Carbon,* Radovic, L. R. (Ed.), **27**, Marcel Dekker, New York, 1 (2001).
7. S. Babel and T. A. Kurniawan, *J. Hazard. Mater.*, **B 97**, 219 (2003).
8. T. K. Naiya, A. K. Bhattacharya and S. K. Das, *Env. Prog.* (2009), DOI:10.1002/ep.10280.
9. W. S. Wan Ngah and M. A. K. M. Hanafiah, *Biosour. Technol.*, **99**, 3935 (2008).
10. H. Xin, G. Nai-yun and Z. Qiao-li, *J. Environ. Sci.*, **19**, 1287 (2007).
11. J. A. Laszlo and F. R. Dintzis, *J. Appl. Polym. Sci.*, **52**, 531 (1994).
12. L. Luduena, D. Fasce, V. A. Alvare and P. M. Stefani, *Bio Resources*, **6**(2), 1440 (2011).
13. L. Linh, U. Eldemerdash, N. Mansor, Y. Uemura and E. Furuya, *Int. J. Biomass Renewables*, **1**(2), 32 (2012).
14. G. H. Sonawane and V. S. Shrivastava, *Desalination*, **247**, 1 430 (2009).
15. M. Ghaedi, H. Hossainian, A. Shokrollahi, F. Shojaipour, M. Soylak and M. K. Purkait, *Desalination*, **281**, 226 (2011).
16. N. Daneshvar, M. Ayazloo, A. R. Khataee and M. Pourhassan, *Bioresour. Technol.*, **98**, 6, 1176 (2007).
17. G. Ciobanu, M. Harja, L. Rusu, A. M. Mocanu and C. Luca, *Korean J. Chem. Eng.*, **31**(6), 1021 (2014).
18. X. Han, X. Niu and X. Ma, *Korean J. Chem. Eng.*, **29**(4), 494 (2012).
19. W. T. Tsai and H. R. J. Chen, *Hazard. Mater.*, **175**(1-3), 844 (2010).
20. T. S. Anirudhan and P. G. Radhakrishnan, *J. Chem. Thermodyn.*, **40**, 702 (2008).
21. Oxford Dictionary of Chemistry, J. Daintith Ed., Oxford University Press (2008).
22. S. Chowdhury, R. Mishra, P. Saha and P. Kushwaha, *Desalination*, **265**, 159 (2011).
23. Y. Subbareddy, V. Jeseentharani, C. Jayakumar, K. S. Nagaraja and B. Jeyaraj, *J. Environ. Res. Dev.*, **7**, 1A (2012).
24. Von Oepen, W. Kördel and W. Klein, *Chemosphere*, **22**, 285 (1991).
25. G. Domínguez, R. Hernández-Huesca and G. Aguilar-Armenta, *J. Mex. Chem. Soc.*, **54**(2), 1161 (2010).
26. S. I. Lyubchik, A. I. Lyubchik and O. L. Galushko, *J. Colloids Surf., A: Physicochem. Eng., Aspects*, **242**(1-3), 151 (2004).